Laser Flash Photolysis Studies of the Kinetics of Reduction of Spinach and *Clostridium* Ferredoxins by a Viologen Analogue: Electrostatically Controlled Nonproductive Complex Formation and Differential Reactivity among the Iron–Sulfur Clusters†

José A. Navarro,‡ Glen Cheddar, and Gordon Tollin*

Department of Biochemistry, University of Arizona, Tucson, Arizona 85721

Received February 21, 1989; Revised Manuscript Received March 30, 1989

ABSTRACT: We have studied the transient kinetics of electron transfer from a positively charged viologen analogue (propylene diquat), reduced by pulsed laser excitation of the deazariboflavin/EDTA system, to the net negatively charged ferredoxins from spinach and *Clostridium pasteurianum*. Spinach ferredoxin showed monophasic kinetics over the ionic strength range studied, consistent with the presence of only a single iron–sulfur center. *Clostridium* ferredoxin at low ionic strength showed biphasic kinetics, which indicates a differential reactivity of the two iron–sulfur centers of this molecule toward the electron donor. The k_{obsd} values for the initial fast phase observed with *Clostridium* ferredoxin were ionic strength dependent, whereas the slow-phase kinetics were ionic strength independent. This correlates with the highly asymmetric charge distribution on the surface of the bacterial protein relative to the two iron–sulfur clusters. The kinetics corresponding to spinach ferredoxin reduction were also ionic strength dependent, and the results obtained with these kinetics and with the fast phase of the bacterial ferredoxin reduction were consistent with a mechanism involving electrostatically stabilized complex formation. For spinach ferredoxin, the second-order rate constant extrapolated to infinite ionic strength was 2-fold smaller, and the extrapolated limiting first-order rate constant was 10-fold smaller, than for *Clostridium* ferredoxin, indicating a smaller intrinsic reactivity of the spinach protein toward the electron donor. Differences in the rate constant values and the ionic strength dependencies with both ferredoxins are consistent with differences in cluster structure and environment and protein size and charge distribution. For both proteins, the total amount of ferredoxin reduced increased with the ionic strength. This can be explained by assuming more than one electrostatic interaction site on the protein, leading to both productive and nonproductive interactions with the electron donor. This explanation is also consistent with effects observed upon the addition of a positively charged polypeptide (polylysine) to the reaction mixture, which decreased the reaction rate constant by competing with the electron donor for the productive site, while increasing the total amount of reduced ferredoxin by also competing for the nonproductive sites. Polylysine had a much smaller effect on *Clostridium* ferredoxin reduction as compared with the spinach protein. This is again consistent with the differences in size and charge distributions of the two proteins.

Ferredoxins are low molecular weight iron–sulfur proteins that play an important role as electron-transfer agents in some fundamental biological systems, such as photosynthesis, respiration, nitrogen fixation, and carbon metabolism (Lovenberg, 1973–1977). They can be divided into two main classes: the lower molecular weight bacterial ferredoxins, usually with eight iron and eight labile sulfur atoms, and the higher molecular weight chloroplast-type ferredoxins, with two iron and two labile sulfur atoms (Thomson, 1985).

Spinach ferredoxin (M_r ~10 500) has a redox-active 2Fe–2S site consisting of a dinuclear cluster represented as $Fe_2S_2(SR)_4$, where SR is a liganded protein cysteinyl sulfur, with a one-electron $E_{m,7}$ = −420 mV. The X-ray structure of the closely related ferredoxin from the blue-green alga *Spirulina platensis* has been established (Fukuyama et al., 1980), and on the basis of a comparison of the amino acid sequence can be assumed to be similar to that of the ferredoxin from spinach (Matsubara et al., 1980). From this structure, it is deduced that the iron–sulfur cluster is located near the surface of the protein and is surrounded by a region having a net negative charge.

The ferredoxin from the bacterium *Clostridium pasteurianum* (M_r ~6000) is known to contain two $Fe_4S_4(SR)_4$ clusters, each one of which can accept or donate one electron with an $E_{m,7}$ = −395 mV. The X-ray structure of the 8Fe ferredoxin from *Peptococcus aerogenes* has been determined (Adman et al., 1973), and on the basis of homologies in the amino acid sequences, a marked structural similarity is also expected between the two bacterial ferredoxins. From this comparison, one can conclude that *Clostridium* ferredoxin is also a net negatively charged protein with a highly asymmetric electrostatic charge distribution. The iron–sulfur clusters are located on opposite sides of the molecule, and most of the negative charges are localized near one of the two clusters, with the other cluster in an essentially uncharged environment.

Several previous kinetic studies have been reported concerning the oxidation and reduction of both ferredoxins. A range of techniques including stopped-flow (Armstrong & Sykes, 1978; Armstrong et al., 1980; Adzamli et al., 1984),

† This research was supported by a fellowship from the Foundation Juan March (Spain) to J.A.N. and by a research grant (DK15057) from the National Institutes of Health to G.T.

* To whom correspondence should be addressed.

‡ Permanent address: Instituto de Bioquímica Vegetal y Fotosíntesis, Universidad de Sevilla y CSIC, Facultad de Biología, Apdo 1113, 41080 Sevilla, Spain.

0006-2960/89/0428-6057$01.50/0

pulse radiolysis (Butler et al., 1979; Maskiewicz & Bielski, 1981; Bowyer et al., 1988), and electrochemical methods (Dasgupta & Ryan, 1982) have been used. The kinetics of electron transfer from reduced ferredoxins to a number of organic complexes (Armstrong & Sykes, 1978; Armstrong et al., 1980) and from reducing agents, such as methyl viologen and metal derivative complexes, to oxidized ferredoxins have been investigated (Dasgupta & Ryan, 1982; Adzamli et al., 1984; Feinberg et al., 1984; Bowyer et al., 1988), including several studies with electrically charged molecules. It has been concluded that in the oxidation and reduction of bacterial ferredoxin the two clusters do not interact, and in fact operate in an independent and identical manner (Butler et al., 1979; Armstrong et al., 1980; Feinberg et al., 1984). However, according to the asymmetric charge distribution, a preferential reactivity toward one of the two clusters would be expected from a positively charged oxidant or reductant. In order to test this, we have carried out a comprehensive series of kinetic comparisons between the spinach and *Clostridium* ferredoxins with respect to electron transfer to these proteins from a positively charged electron donor. Specifically, we have used the viologen analogue 1,1′-propylene-2,2′-bipyridylium radical ($E_{m,7}$ = −550 mV; Steckhan & Kuwana, 1974), also called propylene diquat, which was itself previously reduced by the laser-excited deazariboflavin/EDTA system. The latter has been widely used in our laboratory in the study of the electron-transfer reactions of redox proteins (Bhattacharyya et al., 1983, 1986; Kipke et al., 1988). The viologen analogue has been shown in previous work to be able to mediate the reduction of spinach ferredoxin via electron-transfer quenching of triplet-state chlorophyll in a negatively charged vesicle system (Senthilathipan & Tollin, 1989).

The specific aims of the present study were to compare the reactivities of the two iron–sulfur clusters of *Clostridium* ferredoxin, inasmuch as the positively charged electron donor should be, at low but not at high ionic strength, electrostatically attracted to only one of the two clusters, and to compare the reactivities of the bacterial and higher plant iron–sulfur clusters. This type of investigation also offers the possibility of being able to test for the existence of intramolecular cluster-to-cluster electron transfer in the bacterial ferredoxin. As will be shown below, the properties of both ferredoxins are closely analogous in many aspects, although kinetic differences do exist which can be explained by differences in cluster structure and environment, and in protein size and charge distribution. Moreover, we have evidence that indicates different intrinsic reactivities of the two iron–sulfur centers in the bacterial ferredoxin toward the electron donor. No evidence for intramolecular electron transfer in this ferredoxin has been obtained.

Materials and Methods

Spinach ferredoxin (Fd) was purified according to the method of Borchet and Wessels (1970). Extinction coefficients of 9.7×10^3 and 8.8×10^3 M^{-1} at 420 and 465 nm were used, respectively, to determine the concentration of oxidized Fd (Fd_{ox}). *Clostridium* Fd was purified following the method of Mayhew (1971). An extinction coefficient of 2.7×10^4 M^{-1} at 420 nm was used to determine the Fd_{ox} concentration. The diquat analogue 1,1′-propylene-2,2′-bipyridylium dibromide (PDQ^{2+}) was synthesized by using the procedure of Homer and Tomlinson (1980). The buffer used for the low ionic strength experiments was 5 mM potassium phosphate, pH 7.0, containing 0.6 mM ethylenediaminetetraacetic acid (EDTA), 1.5 mM PDQ^{2+}, and 100 μM 5-deazariboflavin (5-dRf) (I = 21 mM). For high ionic strength experiments, the buffer contained 100 mM potassium phosphate, pH 7.0, 5 mM EDTA, 2 mM PDQ^{2+}, and 100 μM 5-dRf (I = 280 mM). Sodium chloride was added to adjust buffer solutions to the appropriate ionic strengths.

Laser flash photolysis generated 5-deazariboflavin radical (5-dRfH•) which rapidly (<1 μs) underwent electron transfer to PDQ^{2+} to form $PDQ^{+\bullet}$. In the presence of Fd_{ox}, electron transfer from $PDQ^{+\bullet}$ occurred to produce Fd_{red}. All kinetic experiments were performed under pseudo-first-order conditions, in which the concentration of oxidized ferredoxin (>2 μM) was in large excess over the amount of 5-dRfH• (and therefore of $PDQ^{+\bullet}$) radical produced per flash (<0.7 μM). Unless quantitation was required (e.g., for bleaching measurements), the number of flashes per kinetic trace varied. All kinetic traces were analyzed by hand, by fitting to an exponential curve. All kinetic experiments were performed at ambient temperature (23–25 °C) anaerobically in cuvettes which were deaerated by bubbling with water-saturated argon gas. Microliter volumes of a concentrated solution of protein were added via a syringe to the sealed cuvette subsequent to deoxygenation, and resulting traces of oxygen were removed by blowing argon gas across the surface of the solution. Laser photoexcitation was carried out with a nitrogen laser-pumped dye solution (BBQ 2A386 dye from PRA, 396-nm maximum wavelength). A detailed description of the laser flash apparatus and the method of data collection has been published elsewhere (Przysiecki et al., 1985; Bhattacharyya et al., 1983).

In all of the systems investigated, nonlinear ferredoxin concentration dependencies for k_{obsd} values were obtained, implying a mechanism which involved intermediate complex formation [cf. Simondsen et al. (1982)]. The second-order rate constants and the limiting first-order rate constants for ferredoxin reduction were evaluated from these data by a nonlinear least-squares computer-fitting procedure as described previously (Simondsen et al., 1982). The estimated error in these values is ±15%. The ionic strength dependence of the rate constants was fit with a theoretical model for electrostatic interactions, developed by Watkins (1986) and previously described (Tollin et al., 1984; Meyer et al., 1986), to obtain an electrostatically corrected rate constant (k_∞) as well as the electrostatic interaction energy (v_{ii}). Maps of the electrostatic potential on the surface of the ferredoxins were calculated by using the procedure of Matthew (1985) and displayed on an Evans and Sutherland PS390 using the FRODO software package. This method allows calculation of the surface electrostatic potential at different minimum energy levels, corresponding to different kT values, where T is the temperature and k is the Boltzmann constant. Thus, increasing the kT value permits display of only the correspondingly stronger electrostatic potential contour lines.

Results

Reduction of Spinach Ferredoxin by $PDQ^{+\bullet}$. The kinetic trace shown in Figure 1a illustrates the rapid formation by the laser flash of the $PDQ^{+\bullet}$ radical and its subsequent stability under anaerobic conditions in the absence of oxidized protein. The $PDQ^{+\bullet}$ radical has broad light absorption from 450 to 550 nm; kinetic observation of $PDQ^{+\bullet}$ formation and decay was made at 505 nm where the radical has an absorption maximum (Steckhan & Kuwana, 1974). The radical formation process can be represented as follows:

$$5\text{-dRf}_{ox} + e^- \xrightarrow[H^+]{h\nu} 5\text{-dRfH}^\bullet \xrightarrow[PDQ^{2+}]{} 5\text{-dRf}_{ox} + PDQ^{+\bullet} + H^+$$

Ferredoxin reduction was monitored by loss of absorbance at

Table I: Electrostatic Analysis of Ionic Strength Dependence of Electron Transfer from $PDQ^{+\bullet}$ to Ferredoxins[a]

	$k_{12\infty}$ (M^{-1} s^{-1})	v_{ii} (kcal/mol)	Z_2[b]	$k_{23\infty}$ (s^{-1})	v_{ii} (kcal/mol)	Z_2[b]
spinach Fd	1.3×10^9	−2.5	−0.9	2.3×10^3	−4.8	−1.7
Clostridium Fd	2.7×10^9	−3.1	−1.1	2.1×10^4	−1.2	−0.4

[a] In analyzing the rate constant vs ionic strength data, the following parameters were used: ρ (the radius of the active site) = 4.5 Å, r_{12} (the distance between reactants in the intermediate complex) = 3.5 Å, D_e (the dielectric constant within the interaction domain) = 50, and Z_1 (the charge on the reductant) = +1 [see Tollin et al. (1984) for further discussion]. [b] Z_2 is the calculated charge on the reactive site of ferredoxin.

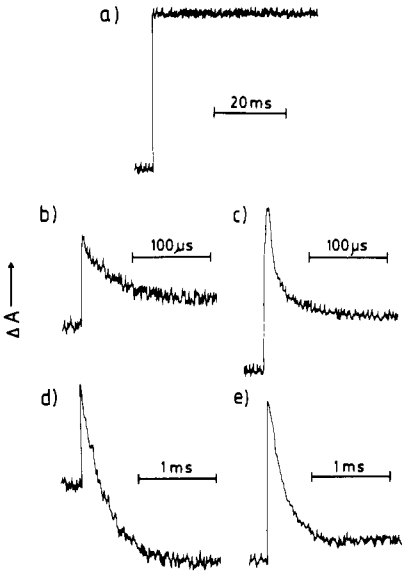

FIGURE 1: Kinetic traces showing the following: (a) $PDQ^{+\bullet}$ radical stability in the absence of protein monitored at 505 nm at I = 21 mM; (b, d) formation of spinach Fd_{red} monitored at 465 nm, I = 21 mM (b) or I = 277 mM (d); (c, e) subsequent $PDQ^{+\bullet}$ oxidation followed at 505 nm, I = 21 mM (c) or I = 277 mM (e). Fd concentration was 10 μM. The buffer conditions were 5 mM potassium phosphate, pH 7.0, 0.6 mM EDTA, 1.5 mM PDQ^{2+}, and 100 μM dRf (I = 21 mM) or 100 mM potassium phosphate, pH 7.0, 5 mM EDTA, 2 mM PDQ^{2+}, and 100 μM dRf (I = 277 mM).

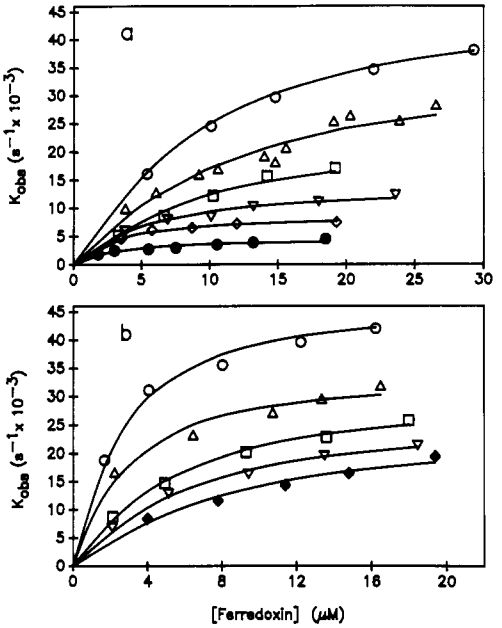

FIGURE 2: Dependence of k_{obsd} for (a) spinach and (b) *Clostridium* ferredoxin reduction by $PDQ^{+\bullet}$ upon protein concentration at different ionic strengths. Solid curves correspond to theoretical fits according to the complex formation mechanism given in the text. The buffer conditions were as described under Materials and Methods. Ionic strength values were as follows: (a) (○) 21 mM; (△) 51 mM; (□) 81 mM; (▽) 141 mM; (◇) 277 mM; (●) 417 mM; (b) (○) 21 mM; (△) 81 mM; (□) 280 mM; (▽) 400 mM; (◆) 680 mM.

465 nm, where the protein has an absorption maximum (Foust et al., 1969) and where overlap with $PDQ^{+\bullet}$ absorbance is low. In the presence of 10 μM Fd_{ox} at both low and high ionic strengths (Figure 1), laser photolysis resulted in an initial rapid increase in absorbance both at 465 nm and at 505 nm. This was followed by an exponential decay that, under some conditions at 465 nm but not at 505 nm, went below the preflash base line. Such changes are consistent with the rapid formation of $PDQ^{+\bullet}$ radical (initial increase) and its subsequent reoxidation (exponential decrease) by Fd_{ox}, leading to the formation of Fd_{red}. Since at 465 nm absorbance changes due to Fd reduction were predominant, the kinetic traces indicate that the amount of protein reduced per laser flash increased with the ionic strength (compare Figure 1b and Figure 1d). The extent of bleaching at 465 nm also increased with the protein concentration (not shown). Protein reduction itself was faster at low ionic strength (compare Figure 1b and Figure 1d). Furthermore, at 505 nm, where absorbance changes due to $PDQ^{+\bullet}$ were predominant, the extent of absorbance decrease due to $PDQ^{+\bullet}$ decay also increased with protein concentration and/or ionic strength (compare Figure 1c and Figure 1e), resulting at high protein concentration and/or ionic strength in an absorbance decay which reached the initial base line. $PDQ^{+\bullet}$ radical reoxidation was also faster at low ionic strengths (compare Figure 1c and Figure 1e). Values of k_{obsd} at both wavelengths were identical within experimental error under all conditions.

The ionic strength and protein concentration dependence for spinach ferredoxin reduction by $PDQ^{+\bullet}$ is shown in Figure 2a. It is evident that the observed rate constants for electron transfer from $PDQ^{+\bullet}$ to Fd_{ox} decreased as the ionic strength increased. Approximate second-order kinetics were observed at low Fd_{ox} concentration, whereas at higher protein concentration the k_{obsd} values for the electron-transfer reaction became relatively independent of Fd concentration.

Inasmuch as spinach Fd is a net negatively charged protein (Matsubara et al., 1980) and the $PDQ^{+\bullet}$ radical is a positively charged electron donor, the ionic strength effects are not unexpected. The individual rate constants can be obtained by a nonlinear least-squares fit of the data to a simple two-step mechanism, in which the reactants initially form an electrostatically stabilized transient complex followed by intracomplex electron transfer and product formation (Tollin et al., 1986). This may be represented as follows:

$$Fd_{ox} + PDQ^{+\bullet} \underset{k_{21}}{\overset{k_{12}}{\rightleftharpoons}} (Fd_{ox}\cdots PDQ^{+\bullet}) \xrightarrow{k_{23}} Fd_{red} + PDQ^{2+}$$

Reverse electron transfer from Fd_{red} to PDQ^{2+} can be ignored because of the relatively large redox potential difference between the redox couples ($\Delta E_{m,7}$ = 136 mV). The solid lines in Figure 2 are the theoretical fits according to this mechanism, and, as is evident, the agreement with the observed values is quite good. Extrapolation of the ionic strength dependence of the k_{12} and k_{23} values to infinite ionic strength (Figure 3a) allows us to obtain an estimate for k_∞ (Table I), which represents the intrinsic rate constant under conditions of negligible electrostatic effects. The data analysis procedure also leads to a value for the electrostatic interaction energy, v_{ii}, which provides information on the strength of the interaction and

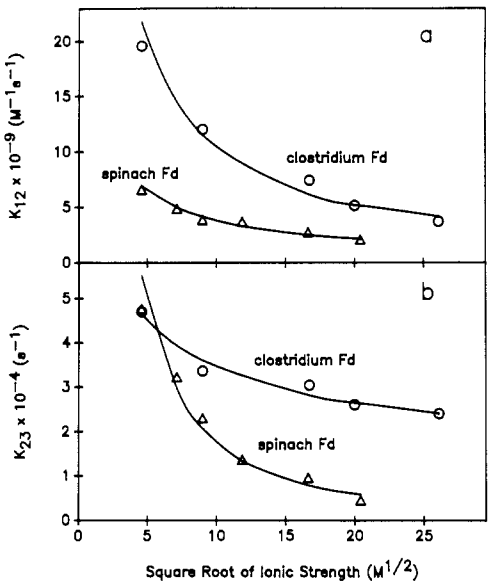

FIGURE 3: Effect of ionic strength on the (a) second- and (b) first-order rate constants for the electron-transfer reactions from $PDQ^{+\bullet}$ radical to ferredoxins.

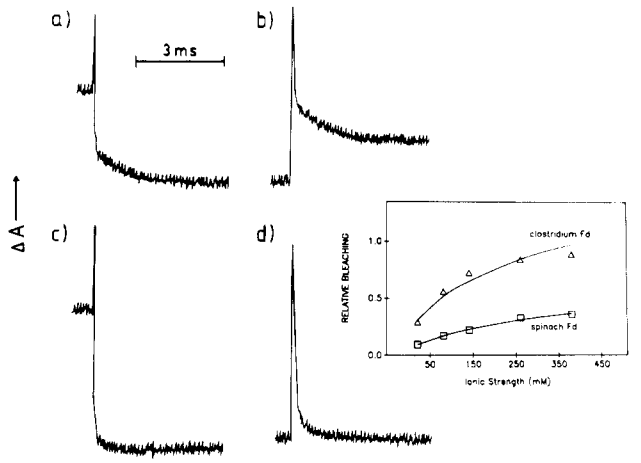

FIGURE 4: Kinetic traces showing the following: (a, c) formation of *Clostridium* Fd_{red} monitored at 465 nm, I = 21 mM (a) or I = 141 mM (c); (b, d) subsequent $PDQ^{+\bullet}$ reoxidation followed at 505 nm, I = 21 mM (b) or I = 141 mM (d). Fd concentration was 8 μM. The buffer conditions were 5 mM potassium phosphate, pH 7, 0.6 mM EDTA, 1.5 mM PDQ^{2+}, 100 μM dRf (I = 21 mM), and an appropriate concentration of NaCl (I = 141 mM). (Inset) Effect of ionic strength on the total bleaching at 465 nm upon laser flash photolysis of dRf–PDQ^{2+}–Fd-containing solutions. Protein concentration was 10 μM (spinach Fd) or 7 μM (*Clostridium* Fd). Solid lines represent theoretical fits as explained in the text.

allows an estimate of the effective active-site charge on the protein (Tollin et al., 1984) (Table I).

Reduction of Clostridium Fd by $PDQ^{+\bullet}$. The laser-induced kinetic traces shown in Figure 4 illustrate the electron-transfer reaction between $PDQ^{+\bullet}$ and *Clostridium* Fd. In the presence of 8 μM Fd_{ox}, laser flash photolysis again resulted in an initial rapid increase in absorbance both at 465 nm and at 505 nm due to $PDQ^{+\bullet}$ radical formation, followed by a further absorbance decay indicating Fd reduction (Figure 4a,c) and $PDQ^{+\bullet}$ reoxidation (Figure 4b,d). Under some conditions, the decay at both wavelengths was biphasic (see below for further discussion). In contrast to the kinetic results for spinach Fd reduction, at low ionic strength the observed bleaching at 465 nm at 8 μM *Clostridium* ferredoxin went below the preflash base line (Figure 4a). Again, the total bleaching increased with the ionic strength (compare Figure 4a,b with Figure 4c,d). The ionic strength dependence of the observed bleaching for both ferredoxins is plotted in Figure 4, inset, where the solid lines again represent theoretical fits according to the electrostatic analysis procedure mentioned above. These theoretical fits lead to v_{ii} values of 3 and 2.5 kcal mol^{-1} for spinach and *Clostridium* Fd, respectively, which are similar to those calculated for the electron-transfer reaction (Table I). Furthermore, ferredoxin reduction and $PDQ^{+\bullet}$ reoxidation again were faster at low ionic strengths (cf. Figures 2 and 4).

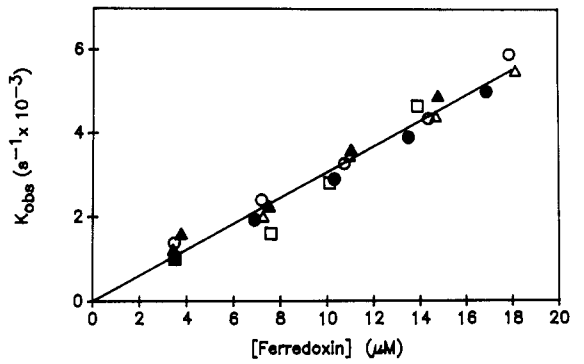

FIGURE 5: Dependence of k_{obsd} for the slow phase of *Clostridium* ferredoxin reduction upon protein concentration at different ionic strengths. The buffer conditions were 2 mM potassium phosphate, pH 7.0, 0.3 mM EDTA, 1 mM PDQ^{2+}, 100 μM dRf (I = 10 mM), and the appropriate concentrations of NaCl. At I = 80 mM, k_{obsd} values were determined by absorbance changes at 505 nm. Ionic strength values were the following: (○) 10 mM; (●) 20 mM; (△) 30 mM; (▲) 40 mM; (□) 80 mM.

The results of the analysis of the ionic strength vs k_{obsd} data (for the fast kinetic phase) are given in Figure 2b and Table I. The electrostatic interaction energy values and the charge on the reactive site of both ferredoxins, obtained from the second-order rate constant data, are similar. In contrast, the values of these parameters obtained from the first-order limiting rate constant (k_{23}) data fit (Figure 3b) are significantly larger in the case of spinach Fd.

Although spinach Fd displayed monophasic kinetics under all conditions, *Clostridium* Fd showed biphasic behavior at low but not at high ionic strength, observed both at 465 nm and at 505 nm (Figure 4a,b). This indicates the occurrence of two different processes in the electron transfer between $PDQ^{+\bullet}$ radical and this latter ferredoxin. In contrast with the fast phase, the slow phase observed for *Clostridium* Fd reduction by $PDQ^{+\bullet}$ was ionic strength independent and k_{obsd} vs concentration plots were linear (Figure 5). From the plot of the k_{obsd} values for this slow phase vs Fd_{ox} concentration, a second-order rate constant of 3.1×10^8 M^{-1} s^{-1} was obtained. Inasmuch as this slow phase become more difficult to observe at 465 nm as the ionic strength increased, it was only possible at high ionic strength (I = 80 mM) to monitor it by following the absorbance changes at 505 nm.

Polylysine Kinetic Effects. We have used an 18-lysine polypeptide for studying the effect that a small, but strongly positively charged, molecule has on the reduction kinetics of both ferredoxins by the positively charged $PDQ^{+\bullet}$ radical. The rationale for these experiments was to determine if the binding between the oppositely charged polypeptides could inhibit the electron transfer from $PDQ^{+\bullet}$ to Fd_{ox}. As expected, polylysine did not produce any effect on the observed kinetic rate constants and observed bleaching at high ionic strength (I = 280 mM) for both ferredoxins (Table II). However, at low ionic strength, polylysine caused a decrease of about 50% in the observed rate constant for the electron transfer between $PDQ^{+\bullet}$ and spinach Fd (Table II). Under these conditions, the ob-

Table II: Effect of Polylysine on Observed Rate Constants for Electron Transfer between $PDQ^{+\bullet}$ and Ferredoxins at Different Ionic Strengths

ionic strength (mM)[a]	k_{obsd} ($s^{-1} \times 10^{-3}$)					
	spinach Fd		*Clostridium* Fd			
	-pLys	+pLys	-pLys[b]	+pLys[b]	-pLys[c]	+pLys[c]
10 (13)	33.9	15.6	45.5	31.1	2.2	2.5
21 (24)	25.2	12.5	39.3	34.7	2.0	2.1
280 (283)	5.7	5.6	19.8	20.0		

[a] Values in parentheses correspond to the ionic strength after addition of polylysine. Polylysine final concentration was 14 μM. [b] Fast phase. [c] Slow phase.

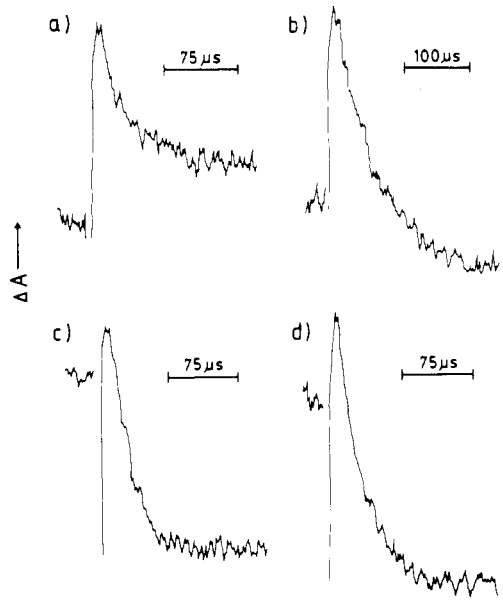

FIGURE 6: Short time scale transient absorbance changes at 465 nm showing (a, b) spinach ferredoxin and (c, d) *Clostridium* ferredoxin reduction by $PDQ^{+\bullet}$ in the absence (a, c) or in the presence (b, d) of polylysine (14 μM). I = 10 mM. Ferredoxin concentration was 8 μM.

served bleaching at 465 nm (Figure 6a,b) and 505 nm (data not shown) increased considerably. In contrast, polylysine addition had only a small effect on the initial fast phase for the *Clostridium* ferredoxin reduction, and also a minor effect on the observed bleaching at 465 and 505 nm (Table II, Figures 6 and 7). At longer times, polylysine addition did not exert any effect on the rate constants corresponding to the slow phase for *Clostridium* Fd reduction (Table II). The effect of polylysine is clearly visible at 465 nm at I = 13 mM but not at I = 21 mM (Figure 7a,c), since the bleaching increase due to the initial phase masked the slower phase at this wavelength. However, the negligible effect of polylysine at I = 21 mM can be easily seen at 505 nm (Figure 7b,c). It should be noted that the polylysine effects cannot be assigned to the ionic strength changes caused by the polypeptide addition, inasmuch as these changes are too small (Table II) to account for the observed results.

Discussion

The laser flash photolysis experiments described above clearly demonstrate a very rapid interaction between the $PDQ^{+\bullet}$ radical and both ferredoxins, k_{obsd} values on the order of 4×10^4 s^{-1} and second-order rate constant values of about 10^9 M^{-1} s^{-1} being obtained at low ionic strength. In the case of spinach Fd, the observed kinetics were shown to be monophasic over the ionic strength range tested, consistent with the existence of only one iron–sulfur cluster per molecule. The

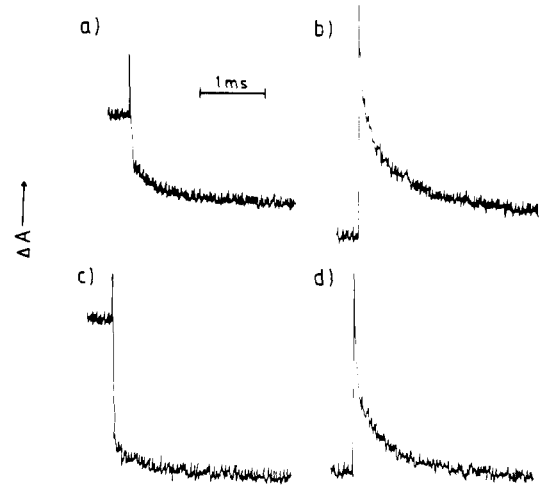

FIGURE 7: Long time scale transient absorbance changes at 465 nm (a, c) or 505 nm (b, d) showing *Clostridium* ferredoxin reduction and $PDQ^{+\bullet}$ oxidation in the absence (a, b) or in the presence (c, d) of 14 μM polylysine. I = 21 mM. Ferredoxin concentration was 8 μM.

ionic strength and nonlinear concentration effects on the kinetic constants for reduction of this protein demonstrated a plus–minus attractive electrostatic interaction between the positively charged electron donor and the negatively charged oxidized ferredoxin, leading to the formation of an electrostatically stabilized transient complex. Similar behavior, i.e., monophasic kinetics of ferredoxin reduction and complex formation, has been reported in a previous work on the spinach ferredoxin reduction by the viologen analogue via electron-transfer quenching of the triplet state of chlorophyll in a lipid vesicle system (Senthilathipan & Tollin, 1989).

The structure of *Spirulina platensis* ferredoxin, as determined by X-ray crystallography, which, on the basis of approximately 70% sequence homology, is likely to be very similar to the ferredoxin from spinach, indicates that the iron–sulfur cluster is located near the molecular surface and is immediately surrounded mainly by uncharged residues. However, several charged residues (principally negatively charged) are found on the protein surface near the cluster, including Arg-42, Glu-94, Glu-95, and Glu-96 and Asp-67, Asp-68, and Asp-69, all of which (except for Glu-96) are conserved in spinach Fd, giving this region a net negative charge (Fukuyama et al., 1980). As can be seen from the electrostatic potentials calculated at various energy levels (Figure 8), the maximum negative potential is localized in a region somewhat to the right of the iron–sulfur cluster (as drawn). Electrostatic interactions have been previously described between spinach as well as other 2Fe–2S ferredoxins and several oxidants and reductants, including in some cases electrostatic complex formation (Armstrong & Sykes, 1978; Adzamli et al., 1983; Bowyer et al., 1988), suggesting that the functional electron-transfer site is close to a significant negative charge. Attractive electrostatic interactions and the relatively large potential difference between $PDQ^{+\bullet}$ and Fd_{ox} ($\Delta E_{m,7}$ = 136 mV) are consistent with the large second-order rate constant values obtained at low ionic strengths for the electron-transfer reaction between these molecules. The present rate constant values are larger than those previously reported for spinach Fd reduction by methyl viologen radical ($MV^{+\bullet}$) as measured with pulse radiolysis (3.7×10^9 M^{-1} s^{-1} vs 8.9×10^7 M^{-1} s^{-1} at $I \sim 100$ mM) (Bowyer et al., 1988). This is consistent with the lower redox potential of PDQ^{2+}. An earlier electrochemical analysis of spinach Fd reduction by $PDQ^{+\bullet}$ gave much smaller values for the second-order rate constant (1.2×10^5 M^{-1} s^{-1}) (Dasgupta & Ryan, 1982). In

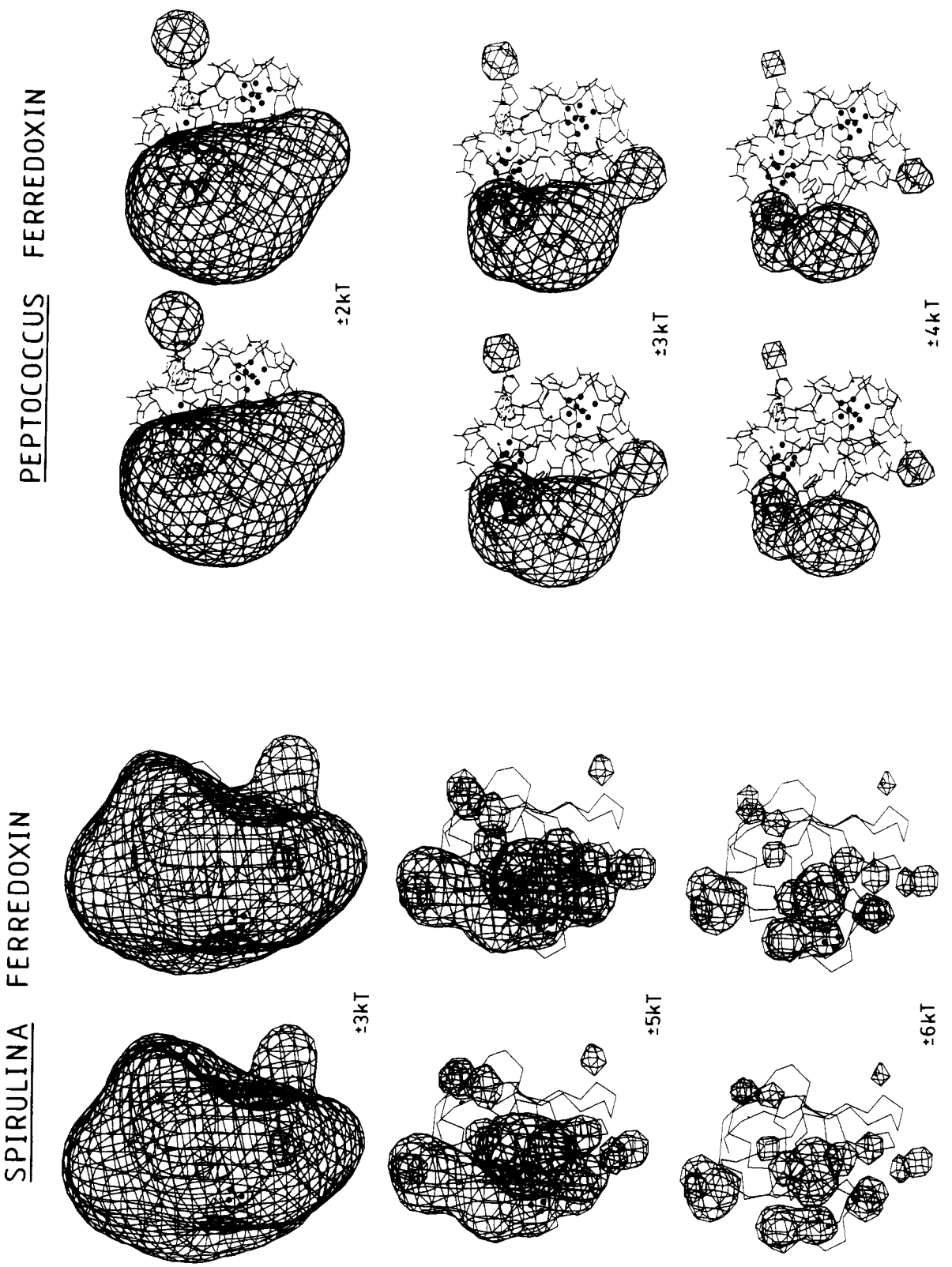

FIGURE 8: Calculated electrostatic potential maps of *Spirulina* and *Peptococcus* ferredoxins. Calculations were made at pH 7.0 and an ionic strength of 20 mM. Solid lines are negative potential, and dashed lines are positive potential. Carbon atom backbones and the iron–sulfur clusters (closed circles) are shown. Maps are displayed at several energy levels for comparison purposes. The *kT* values indicate the minimum energies of contour lines for the electrical potential.

this measurement, processes other than electron transfer must have been rate limiting.

Two kinetically separable optical transients were observed at low ionic strength for *Clostridium* Fd, at both 465 nm and 505 nm, corresponding to Fd reduction and $PDQ^{+\bullet}$ reoxidation. This has not been described previously. Biphasic kinetics toward an electrically charged reductant would be expected from the structure of this ferredoxin, which is approximately 70% homologous to the established *Peptococcus aerogenes* structure. As can be seen in the computer model (Figure 8), *Peptococcus* ferredoxin (and most probably *Clostridium* as well, inasmuch as the charged residues are even more highly conserved between the two proteins than is the total sequence) has a highly asymmetric electrostatic charge distribution. Most of the negative potential is located near one of the two iron–sulfur clusters, with the other one being in an essentially uncharged environment. Thus, a positively charged electron donor should show a preferential reactivity toward one of the two clusters, specifically to the one located in the negatively charged region. The initial faster decay transient behaves qualitatively in the same manner as does spinach Fd reduction (i.e., plus–minus attractive interaction, electrostatic complex formation). Accordingly, it can be assigned to the reaction between the $PDQ^{+\bullet}$ radical and the cluster situated in the negative region of the protein. By contrast, the slower phase was shown to be ionic strength independent, and so it can be assigned to the reaction between the electron donor and the cluster located in the uncharged environment. The intrinsic reactivity of the cluster located in the negative site toward $PDQ^{+\bullet}$ is approximately 10 times greater than is the other cluster, as judged by the k_∞ value of 2.7×10^9 M^{-1} s^{-1} vs a second-order rate constant of 3×10^8 M^{-1} s^{-1}. This is consistent with the fact that the size of the fast phase was appreciably larger than the slow phase under all conditions (cf. Figure 4). We estimate the amplitude ratio between the two phases to be approximately 4:1 at low ionic strength and (10–20):1 based on an extrapolation to infinite ionic strength. The comparison is actually more valid for the infinite ionic strength limit, inasmuch as the extent of bleaching during the fast phase increased with the ionic strength, probably due to a decrease in nonproductive complex formation (see below). Thus, considering the difficulties of the extrapolation procedure, the agreement between the rate constant ratio and the amplitude ratio is not unreasonable.

The disappearance of the biphasic kinetics at higher ionic strength values cannot be assigned to an overlap of both phases caused by the fast phase becoming slower as the ionic strength increased. However, monophasic behavior at high ionic strength can be explained in terms of an increase in the amount of reduced protein produced during the fast phase, as will be discussed further below, which leads to a decrease in the availability of electron donor for the second phase of protein reduction.

The present experiments, to our knowledge, represent the first time that biphasic behavior, and a differential reactivity between the two iron–sulfur clusters, has been observed for *Clostridium* Fd reduction. In previous pulse radiolysis experiments of Fd reduction by e^-_{aq}, $CO_2^{-\bullet}$, and $(CH_3)_2C^{\bullet}OH$, a two-stage electron-transfer mechanism was proposed, with rate constants of 3.4×10^{10} M^{-1} s^{-1} and 1.1×10^3 s^{-1}. However, the second stage was associated with an intramolecular process which generated semireduced Fd for electron transfer from an unidentified portion of the molecule to one of the iron–sulfur clusters (Butler et al., 1979). Thus, the electron-transfer mechanism was complex, which would have made differential reactivities difficult to detect. Stopped-flow studies of the oxidation and reduction of *Clostridium* ferredoxin with a wide variety of metal derivative oxidants and reductants all exhibited monophasic kinetics, despite in many cases large electrostatic effects (Armstrong et al., 1980; Adzamli et al., 1984). For all of these reactions, it was assumed that both iron–sulfur centers reacted in an equivalent and independent manner. However, the comparatively small rate constant values obtained in these studies (10^3–10^4 M^{-1} s^{-1} vs 10^9–10^{10} M^{-1} s^{-1}), and the large excess concentration of oxidants or reductants which were used, could have masked possible biphasic behavior.

The larger k_∞ values for both the first- and the second-order reactions obtained with *Clostridium* Fd compared with spinach Fd (Table I) indicates a higher intrinsic reactivity of this ferredoxin toward the electron donor. Similar behavior has been reported in the reactions between a positively charged chromium macrocycle complex reductant and parsley and *Clostridium* ferredoxins, with a 7 times higher reactivity obtained for the bacterial Fd as compared with the one from parsley (Adzamli et al., 1984). Such a result would not be expected on an energetic basis, inasmuch as in both cases the thermodynamic driving force, the electrostatic interaction energy, and the charge on the reactive sites are similar (Table I). Therefore, other factors, e.g., structural and steric effects, have to play a major role in causing this difference. This deserves further investigation.

The bleaching increase observed for both proteins at high ionic strength (even though the k_{obsd} values are smaller) suggests an increase in the total amount of reduced protein. This effect (observed both at 465 nm and at 505 nm) can be explained by assuming a decrease in the *effective* concentration of one of the reactants at low ionic strength values, i.e., a diminution either in the amount of $PDQ^{+\bullet}$ radical formation or in the amount of reactive ferredoxin, leading in either case to a decrease in protein reduction. The initial flash-induced absorbance changes observed at 505 nm do not indicate any differences in the amount of $PDQ^{+\bullet}$ radical produced as the ionic strength changes, which points to effects related to protein reactivity. One possibility in the latter category is a salt-induced ferredoxin conformational change (perhaps accompanied by a change in the redox potential) resulting in a nonreactive form of the protein at low ionic strength. However, no changes in the absorption spectra of either ferredoxin have been detected over the ionic strength range used here. On the other hand, previous laser flash photolysis experiments involving spinach Fd reduction by $dRfH^{\bullet}$ radical itself (Bhattacharyya et al., 1986) showed an increase in the second-order rate constants at higher ionic strength values, even though no electrostatic effects were expected since the $dRfH^{\bullet}$ radical is electrically neutral. However, changes in the extent of bleaching were not detected in this study. If two different forms of ferredoxin exist simultaneously at low ionic strength, one of them must be completely unreactive toward $PDQ^{+\bullet}$; otherwise, biphasic ionic strength dependent kinetics should have been observed.

A second possibility which can account for these results is the existence on the surface of both ferredoxins of more than one electrostatic interaction site. According to the structure of both proteins (cf. Figure 8), negatively charged regions are located on the surface of these molecules away from the iron–sulfur clusters. A nonproductive interaction between the positively charged electron donor and these sites could lead to an effective decrease in the $PDQ^{+\bullet}$ available for the electron-transfer reaction to the clusters, resulting in an observed

decrease in the total amount of protein being reduced. If the strengths of the electrostatic interactions were comparable for the productive and nonproductive complexes, the ionic strength increase would diminish the nonproductive interactions, thereby increasing the amount of ferredoxin reduction, while at the same time decreasing the second-order rate constant of the reaction. The similar v_{ii} values obtained for the two effects support this interpretation. The existence of more than one electrostatic interaction site correlates well with the smaller observed bleaching of spinach Fd compared with *Clostridium* Fd at the same ionic strength, and also with the smaller increase of the bleaching observed with the higher plant protein as the ionic strength increased (Figure 4, inset). Thus, spinach Fd is a larger protein ($M_r \sim 10.5$K) than is *Clostridium* Fd ($M_r \sim 6$K) and has a larger fraction of its surface covered by negative electrostatic potential (cf. Figure 8), leading to the possible occurrence of more nonproductive interactions with the $PDQ^{+\bullet}$ radical.

The ionic strength dependence of the second-order rate constant is similar in both ferredoxins, as evidenced by the similar calculated values for the electrostatic interaction energy and the charge on the reactive sites (Table I). On the other hand, ionic strength exerts a much larger effect on the limiting-first order rate constant for spinach Fd reduction as compared with the bacterial protein. Furthermore, the k_∞ values for this constant are 10 times smaller in the case of the higher plant Fd, although similar values were observed at low ionic strength. The ionic strength dependence of this limiting rate constant can be assumed to reflect the extent of nonproductive (or less productive) interactions between the electron donor and both proteins [cf. Bhattacharyya et al. (1986)]. Since, as noted above, spinach Fd would be expected to have a greater number of possible nonoptimal sites for electron transfer, this would result in a smaller value for the infinite ionic strength limiting rate constant, and a larger v_{ii} value for nonoptimal interactions. We consider an interpretation based on nonproductive complex formation to be the most likely one, although conformational effects cannot be completely ruled out at this time. Furthermore, as will be seen below, this mechanism also allows a simple explanation for some of the results obtained with polylysine.

Polylysine exerts a sizable effect on the reduction of spinach Fd, decreasing the rate constants for this reaction at the same time that it increases the observed bleaching. This means that polylysine binding to this protein must exert a dual action. First, it decreases the reaction rate constant by competing with $PDQ^{+\bullet}$ for the reactive site, and, second, it increases the total amount of reduced ferredoxin by competing with the electron donor radical for the nonproductive sites. Consistent with this interpretation, polylysine has a much smaller effect on the *Clostridium* Fd reduction. Only at very low ionic strength ($I = 10$ mM) was it possible to observe a significant decrease in the rate constant for the electron-transfer reaction and a relatively small bleaching increase with the *Clostridium* protein. This can again be explained by the different size and charge distribution of both proteins, leading to a stronger electrostatic interaction between polylysine and spinach Fd, and thus to a stronger competition with $PDQ^{+\bullet}$ both for the reactive and for the nonproductive sites.

In summary, by using a positively charged electron donor as a probe, we have demonstrated large effects of electrostatic charges on the surface of a higher plant and a bacterial ferredoxin on the kinetics of electron transfer. These are a consequence of complex formation between the reactants, in both productive and nonproductive modes, and, in the case of the bacterial ferredoxin, to differential reactivity between the two iron–sulfur centers. Furthermore, by extrapolation of rate constant values to infinite ionic strength, differences in the intrinsic reactivities of the various iron–sulfur clusters toward the reductant became apparent. Such differences are probably not thermodynamic in origin (i.e., based on redox potential effects) but rather reflect as yet uncharacterized effects due to structural, steric, and environmental differences between the redox sites. These features require further study.

Registry No. Propylene diquat cation radical, 121013-72-7.

References

Adman, E. T., Sieker, L. C., & Jensen, L. H. (1973) *J. Biol. Chem. 248*, 3987–3996.

Adzamli, I. K., Petrou, A., Sykes, A. G., Rao, K., & Hall, D. O. (1983) *Biochem. J. 211*, 219–226.

Adzamli, I. K., Henderson, R. A., Sinclair-Day, J. D., & Sykes, A. G. (1984) *Inorg. Chem. 23*, 3069–3073.

Armstrong, F. A., & Sykes, A. G. (1978) *J. Am. Chem. Soc. 100*, 7710–7715.

Armstrong, F. A., Henderson, R. A., & Sykes, A. G. (1980) *J. Am. Chem. Soc. 102*, 6545–6551.

Bhattacharyya, A. K., Tollin, G., Davis, M., & Edmondson, D. E. (1983) *Biochemistry 22*, 5270–5279.

Bhattacharyya, A. K., Meyer, T. E., & Tollin, G. (1986) *Biochemistry 25*, 4655–4661.

Borchet, M. T., & Wessels, J. S. C. (1970) *Biochim. Biophys. Acta 197*, 78–83.

Bowyer, J. R., O'Neill, P., Camilleri, P., & Todd, Ch. M. (1988) *Biochim. Biophys. Acta 932*, 124–129.

Butler, J., Henderson, R. A., Armstrong, F. A., & Sykes, A. G. (1979) *Biochem. J. 183*, 471–474.

Dasgupta, S. R., & Ryan, M. D. (1982) *Biochim. Biophys. Acta 680*, 242–249.

Feinberg, B. A., Tuschel, D. D., & Ryan, M. D. (1984) *Bioelectrochem. Bioenerg. 12*, 575–581.

Foust, G. P., Mayhew, S. G., & Massey, V. (1969) *J. Biol. Chem. 244*, 964–970.

Fukuyama, K., Hase, T., Matsumoto, S., Tsukihara, T., Katsube, Y., Tanaka, N., Kakudo, M., Wada, K., & Matsubara, H. (1980) *Nature 286*, 522–524.

Homer, R. F., & Tomlinson, T. E. (1980) *J. Chem. Soc.*, 2498–2503.

Kipke, C. A., Cusanovich, M. A., Tollin, G., Sunde, R. A., & Enemark, J. (1988) *Biochemistry 27*, 2918–2926.

Lovenberg, W., Ed. (1973–1977) *Iron–Sulphur Proteins*, Vol. I–III, Academic Press, New York.

Maskiewicz, R., & Bielski, K. J. (1981) *Biochim. Biophys. Acta 638*, 153–160.

Matsubara, H., Hase, T., Wakabayashi, S., & Wada, K. (1980) *UCLA Forum Med. Sci. 21*, 245–266.

Matthew, J. B. (1985) *Annu. Rev. Biophys. Chem. 14*, 387–417.

Mayhew, S. G. (1971) *Biochim. Biophys. Acta 235*, 289–302.

Meyer, T. E., Cheddar, G., Bartsch, R. G., Getzoff, E. D., Cusanovich, M. A., & Tollin, G. (1986) *Biochemistry 25*, 1383–1390.

Przysiecki, C. T., Bhattacharyya, A. K., Tollin, G., & Cusanovich, M. A. (1985) *J. Biol. Chem. 260*, 1452–1458.

Senthilathipan, V., & Tollin, G. (1989) *Photochem. Photobiol. 49*, 345–348.

Simondsen, R. P., Weber, P. C., Salemme, F. R., & Tollin, G. (1982) *Biochemistry 21*, 6366–6375.

Steckhan, E., & Kuwana, T. (1974) *Ber. Bunsen-Ges. Phys. Chem. 78*, 253–259.

Thomson, A. J. (1985) in *Metalloproteins* (Harrison, P., Ed.) Part 1, pp 78–121, Verlag Chemie, Weinheim.
Tollin, G., Cheddar, G., Watkins, J. A., Meyer, T. E., & Cusanovich, M. A. (1984) *Biochemistry 23*, 6345–6349.
Tollin, G., Meyer, T. E., & Cusanovich, M. A. (1986) *Biochim. Biophys. Acta 853*, 29–41.
Watkins, J. A. (1986) Ph.D. Thesis, University of Arizona, Tucson, AZ.

Refined Crystal Structure of Cytoplasmic Malate Dehydrogenase at 2.5-Å Resolution†

Jens J. Birktoft,* Gale Rhodes,‡ and Leonard J. Banaszak§

Department of Biological Chemistry, Division of Biology and Biomedical Sciences, Washington University School of Medicine, St. Louis, Missouri 63110

Received December 15, 1988; Revised Manuscript Received March 21, 1989

ABSTRACT: The molecular structure of cytoplasmic malate dehydrogenase from pig heart has been refined by alternating rounds of restrained least-squares methods and model readjustment on an interactive graphics system. The resulting structure contains 333 amino acids in each of the two subunits, 2 NAD molecules, 471 solvent molecules, and 2 large noncovalently bound molecules that are assumed to be sulfate ions. The crystallographic study was done on one entire dimer without symmetry restraints. Analysis of the relative position of the two subunits shows that the dimer does not obey exact 2-fold rotational symmetry; instead, the subunits are related by a 173° rotation. The structure results in a R factor of 16.7% for diffraction data between 6.0 and 2.5 Å, and the rms deviations from ideal bond lengths and angles are 0.017 Å and 2.57°, respectively. The bound coenzyme in addition to hydrophobic interactions makes numerous hydrogen bonds that either are directly between NAD and the enzyme or are with solvent molecules, some of which in turn are hydrogen bonded to the enzyme. The carboxamide group of NAD is hydrogen bonded to the side chain of Asn-130 and via a water molecule to the backbone nitrogens of Leu-157 and Asp-158 and to the carbonyl oxygen of Leu-154. Asn-130 is one of the corner residues in a β-turn that contains the lone cis peptide bond in cytoplasmic malate dehydrogenase, situated between Asn-130 and Pro-131. The active site histidine, His-186, is hydrogen bonded from nitrogen ND1 to the carboxylate of Asp-158 and from its nitrogen NE2 to the sulfate ion bound in the putative substrate binding site. In addition to interacting with the active site histidine, this sulfate ion is also hydrogen bonded to the guanidinium group of Arg-161, to the carboxamide group of Asn-140, and to the hydroxyl group of Ser-241. It is speculated that the substrate, malate or oxaloacetate, is bound in the sulfate binding site with the substrate 1-carboxyl hydrogen bonded to the guanidinium group of Arg-161.

The malate dehydrogenases (malate dehydrogenase, L-malate:NAD oxidoreductase, EC 1.1.1.37)[1] are oxidoreductases that interconvert the substrates malate and oxaloacetate utilizing the NAD/NADH cofactor system. In eukaryotic cells, malate dehydrogenase occurs in two forms, both of which are synthesized in the cytoplasm. After synthesis the mitochondrial form is imported into the mitochondrial matrix (Chen & Freeman, 1984), a process that is facilitated by a translocation sequence (Grant et al., 1986). The cytoplasmic form, sometimes called soluble malate dehydrogenase, remains in the cytoplasm after synthesis as an N-terminal acetylated product. Both forms of malate dehydrogenase are homodimers with molecular masses of 2 × 35 and 2 × 33 kDa for the cytoplasmic and mitochondrial forms, respectively.

Cytoplasmic malate dehydrogenase was among the first oligomeric enzymes to have its three-dimensional structure determined at high resolution (Hill et al., 1972; Webb et al., 1973). Even though the amino acid sequence remained undetermined for a period of time, a number of significant conclusions could be reached regarding its structure–function relationships as well as evolutionary relationships to other nucleotide binding proteins (Webb et al., 1973; Banaszak & Webb, 1975; Birktoft & Banaszak, 1983; Birktoft et al., 1982a,b).

Recently the determination of the amino acid sequence of cMDH has been completed, by a combination of X-ray and chemical methods (Birktoft et al., 1987; Bradshaw et al., 1988).[2] With this information in hand, the restrained, least-squares refinement initiated in the absence of a complete amino acid sequence (Birktoft et al., 1982b) was continued. While this refinement was in progress, a partial cDNA nucleotide sequence for porcine cMDH was reported (Joh et al.,

† This work was supported by NSF Grant PCM-8208894 (L.J.B.) and National Institutes of Health biomedical research support grant to Washington University School of Medicine (J.J.B.).

* Address correspondence to this author at the Department of Biological Chemistry, Washington University School of Medicine, 660 South Euclid Ave., Box 8094, St. Louis, MO 63110.
‡ Present address: Department of Chemistry, University of Southern Maine, 96 Falmouth St., Portland, ME 04103.
§ Present address: Department of Biochemistry, University of Minnesota, Minneapolis, MN 55455.

[1] Abbreviations: rms, root mean square; cMDH, cytoplasmic malate dehydrogenase; mMDH, mitochondrial malate dehydrogenase.

[2] J.-K. Fang, M. J. Wade, B. E. Glatthaar, M. R. Sutton, G. R. Barbarash, G. A. Grant, and R. A. Bradshaw, unpublished results. R. A. Bradshaw, J.-K. Fang, R. T. Fernley, J. J. Birktoft, and L. J. Banaszak, unpublished results.

0006-2960/89/0428-6065$01.50/0